Aero-Structural Design Optimization of Composite Wind Turbine Blade

Naishadh G. Vasjaliya[1] and Sathya N. Gangadharan[2]

[1]Graduate Student, Department of Aerospace Engineering
Embry-Riddle Aeronautical University
Daytona Beach, Florida, USA
naishadh_29@yahoo.com

[2]Professor, Department of Mechanical Engineering
Embry-Riddle Aeronautical University
Daytona Beach, Florida, USA
sathya@erau.edu

Abstract

A multidisciplinary design optimization (MDO) process is defined for a SERI-8 wind turbine blade to optimize its aerodynamic and structural performance. The objective behind this research is to develop a fluid-structural interaction (FSI) system for SERI-8 composite blade to maximize aerodynamic efficiency and structural robustness while reducing blade mass and cost. In the previous research, a MDO process of a composite wind turbine blade has been pioneered as effective process to develop structurally optimized blade design. A multidisciplinary design optimization process is defined in conjunction with structural and aerodynamic performance of the blade. The composite wind turbine blade MDO is divided into three steps and the design variables considered are related to the shape parameters, twist distributions, pitch angle and the relative thickness based on number of composite layers. The constraints are tip deformations and allowable stresses. The results of the first step are aerodynamically optimal twist angles of airfoils for the blade cross-sections along the blade span wise direction, and the pressure distribution along the blade at maximum lift and wind conditions. Airfoil performance is predicted with XFOIL/Qblade, while CFD analysis is performed by CFX software. The second step yields optimal material, composite layup distribution of the blade and involves structural analysis for transferred pressure load from CFD analysis. A parameterized finite element model of the blade is created using ANSYS design modeler/meshing and ACP composite prepost is used to define composite layups of the blade. At the last step, the results of the CFD and the structural analysis are transferred to ANSYS design explorer; accompanied by the cost estimation for the optimization process. The number of design of experiments (DOEs) is defined by Central Composite Design-G optimality method and response surface is created. With the consideration of maximum power output and minimum weight, an optimal blade design was found within the pre-defined design variable parameters and structural constraints. Sensitivity analysis is also performed to observe the impact of input parameters on output parameters for enhanced control of the MDO process.

Keywords: Aero-Structural Optimization, Wind Turbine, Composite Structures, Multi-Objective design Optimization, Fluid Structure Interaction, Computational Fluid Dynamics.

1. Introduction

Wind turbines have become an economically competitive form of clean and renewable power generation. In the United States and abroad, the wind turbine blades continuing to be the target of technological improvements by the use of highly effective and productive design, materials, analysis, manufacturing and testing. Wind energy is a low density source of power [1]. To make wind power economically feasible, it is important to maximize the efficiency of converting wind energy into mechanical energy. Among the different aspects involved, rotor aerodynamics is a key determinant for achieving this goal. There is a tradeoff between aerodynamic efficiency (thin airfoil) and structural efficiency (thick efficiency) both of which have a strong effect on the cost of electricity generated. The design process for optimum design therefore requires determining the optimum thickness distribution by finding the effect of blade shape and varying thickness on both the power output and the structural weight.
Due to the development of computer aided design tools, the design, analyses and manufacturing of wind turbine blades were made very cost effective and feasible. Aerodynamics performance of wind turbine blades can be analyzed using computational fluid dynamics (CFD).The finite element method (FEM) can be used for the blade

structural analysis. Numerical methods have become very practical and widely used to find optimal design of wind turbine blades.

At present, wind turbines are more powerful than early versions and employ sophisticated materials, electronics and aerodynamics [2]. Costs have declined, making wind more competitive clean energy source with other power generation options. Designers apply optimization tools for improving performance and operational efficiency of wind turbines, especially in early stages of product development. The main aim of this research is to present some fundamental issues concerning design optimization of the main wind turbine structures, practical realistic optimization models using different strategies for enhancing blade aerodynamics, structural dynamics, robustness, and aero elastic performance. A number of structural and aerodynamic design variables are presented in order to acquire an optimal blade design which gives higher power output with minimum cost and weight in conjunction with necessary structural constraints.

The objective behind this research work was to evaluate multidisciplinary optimization process for the wind turbine. By creating a Fluid-Structure Interaction (FSI) systems to evaluate structural robustness based on aerodynamic performance and physical wind impact on the blade; and enhance blade performance. The Qblade/XFOIL [3] was used to calculate 2D performance of airfoils and new angle of attack (AOA) defined to modify SERI-8 blade. A 3D modeling software CATIA [4] was employed to design blade geometry and imported into the ANSYS workbench which provides interconnectivity between different structural, aerodynamic analysis modules and design optimization tools. The SERI-8 wind turbine blade is a reference blade design and modified for better aerodynamic performance. The aerodynamic effects calculated using CFX module and the stresses can be determined by mapping pressures on blade by FSI. In the process of optimization, structure and aerodynamic design variables were set as an input parameters and number of DOEs (Design of Experiments) were created and solved. The multidisciplinary optimization process was defined with multiple objectives such as, maximize power, minimize cost and minimize weight within given constraint limits to obtain aero-structural optimal blade design.

2. Governing Principle of Wind Turbine Blade

The principle behind the operation of the wind turbine for generating power from the forces of nature is a revolutionary one. The blades harness the energy from the wind by rotation depending on the wind force applied and the direction of the wind. The wind turbine blade geometry plays vital role in power generation process.

2.1 Blade Selection

The most important part in designing a wind turbine is the blade and the choice of airfoils used at various sections of the blade. The lift generated from these airfoils causes the rotation of the blade and performance of the blade is highly depended of airfoils performance. For this research, SERI-8 wind turbine blade was selected.

2.2 SERI-8 / Airfoil Family

The SERI-8 was originally designed by the Solar Energy Research Institute (SERI), now called the National Renewable Energy laboratory, (NREL) in 1984. The SERI-8 blade is 7.9 m long and has a set of airfoils S806A, S806A, S807, S808 airfoils which were designed for medium size turbines rated at 20-100 kW. The airfoils closer to the tip of the blade generate higher lift due to the speed variation in the relative wind. The purpose of the airfoils at the root of blade is mainly structural, contributing to the aerodynamics performance of the blade but at a lower level. Thus the root of the blade is bigger and stronger than its tip.

Ong and Tsai [5] evaluated the benefits of carbon fibers in a wind turbine blade compared to initial glass/epoxy composite material and studied cost effective model for SERI-8[1]. Jin Woo Lee [6] developed a multidisciplinary optimization process to find maximum blade length for the SERI-8 by minimizing the cost based on annual power generation and maximized the profit. In previous research on SERI-8, static analysis was performed based on predicted aerodynamic pressure load on the blade, which does not replicate real wind turbine loading conditions. Hence, computational fluid dynamics (CFD) analysis is required. There is a need to predict performance of the blade at different wind conditions as well as to study the effect of lift-drag coefficients, pressure distribution along the blade and turbulence on the blade performance.

2.3 Baseline SERI-8 Blade Design

The SERI-8 blade is shown in Figure 1. The SERI-8 blade is 7.9 m long and was divided into 13 equal sections. The twist axis is located at 30% of chord and the blade geometry. The detail of each section and their variables are given in Table 1. The SERI-8 has two ribs at 60 inch and 252 inch locations from the root, which were not considered in

the present research. The geometry data of SERI-8 was found in Ong and Tsai [5]. The baseline design of SERI-8 blade was designed in CATIA v5R20 based on the data provided and imported into the ANSYS design modeler as *.stp* file.

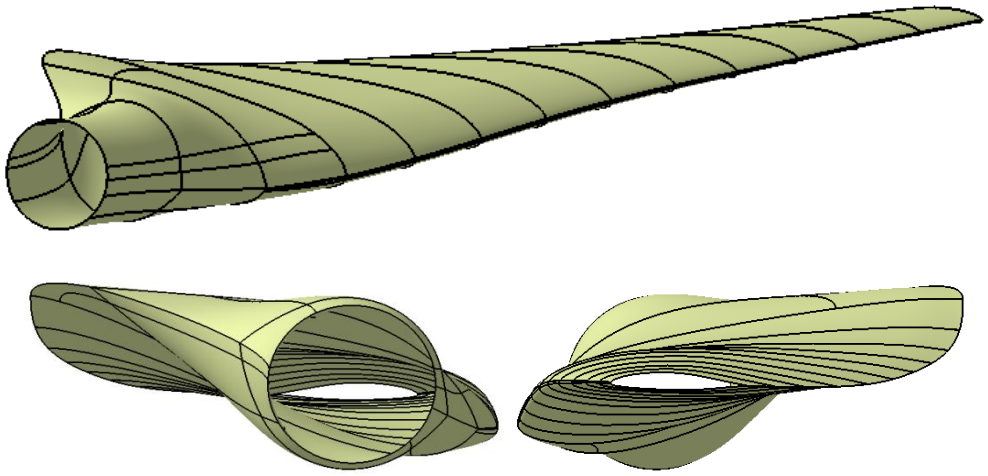

Figure 1: CATIA model of SERI-8 blade

Table 1: SERI-8 blade section geometry

Station	Blade location (inch)	Rotor Radius (inch)	(m)	Chord (inch)	Twist angle (degree)	Airfoils
1	12	37	0.9398	17.83	0	Circle
2	36	61	1.5494	29.43	0	Circle
3	60	85	2.159	44	20	S808
4	84	109	2.7686	43.09	14.81	S807
5	108	133	3.3782	41.42	10.61	
6	132	157	3.9878	39.27	7.29	
7	156	181	4.5974	36.71	4.74	S805A/S807
8	180	205	5.207	33.81	2.87	
9	204	229	5.8166	30.61	1.57	
10	228	253	6.4262	27.13	0.74	S805A
11	252	277	7.0358	23.38	0.27	S805A/S806A
12	276	301	7.6454	19.4	0.06	
13	300	325	8.255	15.19	0	S806A

3. Approach

3.1 Modified SERI-8 Blade

3.1.1 2D Airfoils Performance with Qblade/XFOIL

Qblade/XFOIL is a coupled panel method/boundary layer code that is often used in the wind energy community to evaluate airfoil performance parameters. XFOIL uses an e^N method for transition prediction and is widely used for predicting performance characteristic on 2D airfoils. To predict an angle of attack for higher C_l/C_d ratio for individual airfoils, all airfoils were analyzed at Reynolds number in the range $5x10^5$ to $1x10^6$ and angle of attack in the range 0^0 to 30^0.

The Figure 2 shows C_l versus AOA (0^0 to 30^0) graph of all SERI-8 airfoils. It can be observed that for a higher angle of attack, the lift coefficient increases up to a point where the airfoils experience stall and thus indicates a sudden drop in the graph. It can also be seen that a higher lift is achieved by airfoil S808 which is thicker and has greater camber.

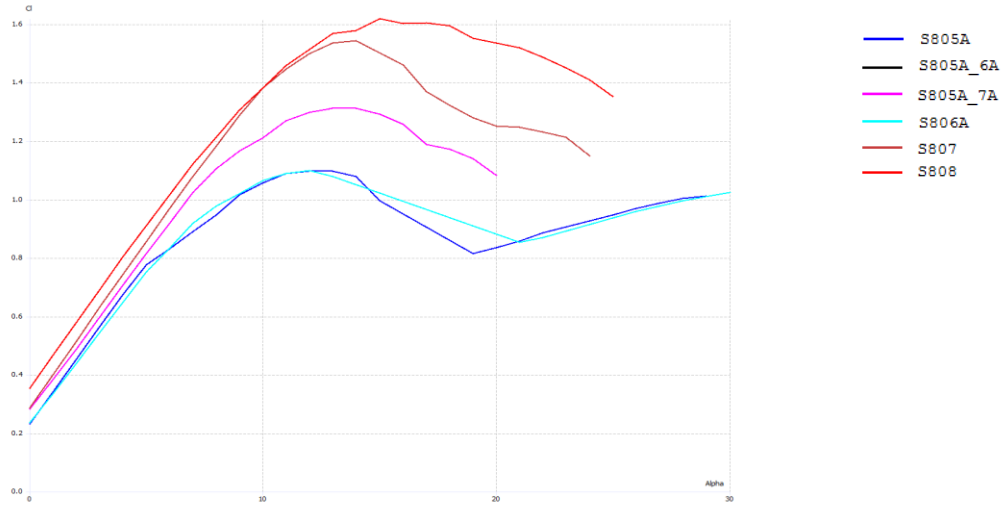

Figure 2: C_l versus AOA

C_l/C_d ratio versus AOA plot is shown in Figure 3. It is interesting to note that the C_l/C_d is higher for the S806A airfoil located at the tip of the blade. Although the other airfoils have higher lift, they also generated more drag given the higher camber. Therefore C_l/C_d ratio is increased from the root to the tip region of the blade. The performance of a wind turbine is improved by increasing the rotational speed, and hence the torque of the rotating blades. If the Cl/C_d is higher in the tip region, a higher torque is generated for the wind turbine.

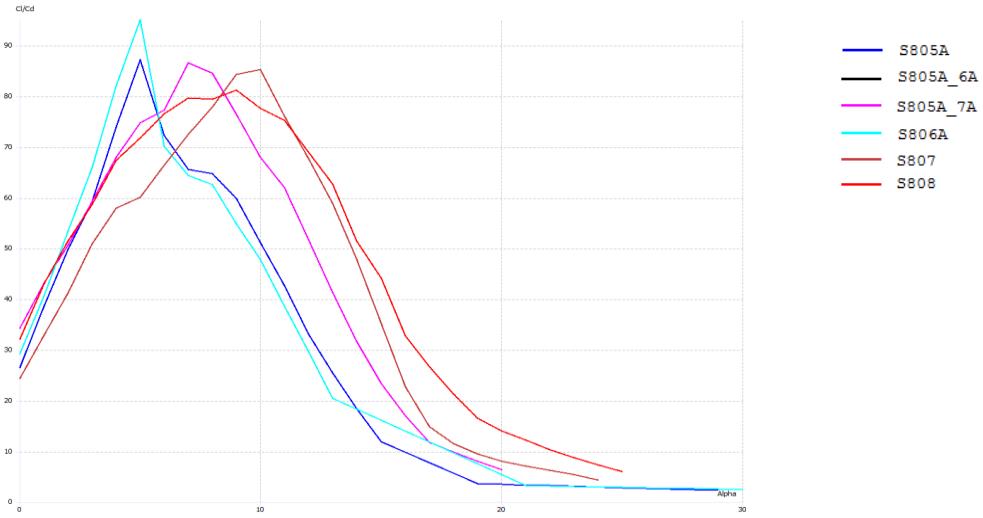

Figure 3: C_l/C_d ratio versus AOA

The AOA of airfoils in the baseline SERI-8 design are provided in Table 2. These are not the angle of attack values for maximum C_l and C_l/C_d ratio calculated from 2D airfoil analysis (Figure 2 and Figure 3). It can be said that the AOA assigned to the baseline SERI-8 design may not the optimum angle of attack. By replacing the baseline SERI-8 airfoils with an angle that provides a higher lift coefficient (C_l) as well as higher C_l/C_d ratio value, more lift force can

be generated. It is not practical to predict and expect similar outcomes for a 3D blade based on 2D airfoil analysis. Based on maximum lift coefficient and maximum C_l/C_d with respect to AOA for individual airfoils, a new SERI-8 blade was developed to produce better aerodynamic performance compared to the baseline SERI-8 design. The twist angles for new SERI-8 are shown in Table 2.

Table 2: Twist angles for SERI-8 and modified SERI-8 airfoils

Airfoils	S808	S807	S805A_7A	S805A	S805A_6A	S806A	
SERI-8	20	13.93	4.359	0.635	0.105	0	Angle (°)
New SERI-8 (Qblade)	18	13.5	7	4.5	0.20	0	

3.2 Pressure Distribution

In order to examine aerodynamic performance of the baseline SERI-8 and new SERI-8 blades, the pressure coefficient plots of airfoils were generated in Qblade. All calculations were made assuming incompressible flow and a Reynolds number of $1x10^6$.

Pressure distribution plots of airfoils at the angle of attack used in baseline SERI-8 are shown in Figure 4. The pressure distribution of airfoils at modified angle of attack for new SERI-8 is shown in Figure 5. Airfoils S808, S807 and S806A angle of attack is not different than the baseline SERI-8 blade. Therefore, the C_p plots look similar and the pressure difference between pressure and suction side surfaces is almost ideal. However, airfoils S805A_7A and S805A in new SERI-8 indicate larger pressure coefficient difference between suction and pressure side with smooth flow translation as well as no flow separation along the chord length compared to the baseline SERI-8, which indicates that a higher torque can be generated. Similarly, S805A_6A airfoil in new SERI-8 has better pressure distribution with higher angle of attack compared to the baseline design and has attached flow till the trailing edge. However, XFOIL appears to over predict the flow separation and fully turbulent computation does not capture this phenomenon. Hence a 3-D CFD simulation is required to validate and compare the aerodynamic performance [7].

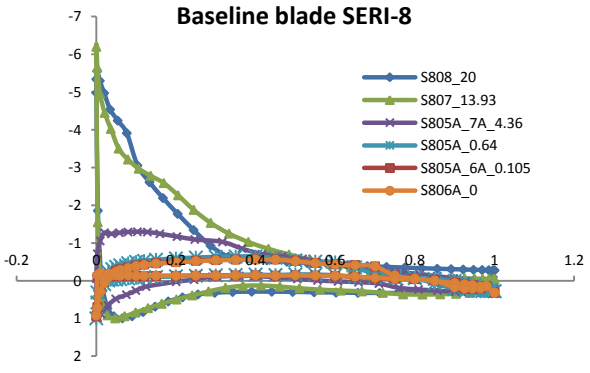

Figure 4: Baseline SERI-8 airfoils C_p plots

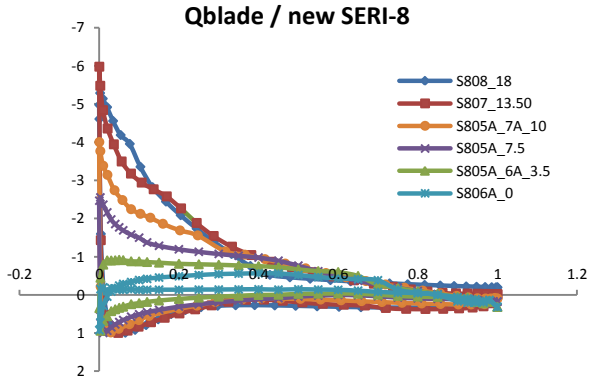

Figure 5: New SERI-8 airfoils C_p plots

3.3 Composite Material

Majority of wind turbine blades is made of fiberglass material and reinforced with polyester or epoxy resin. The materials used for SERI-8 blade design were same as that of Ong and Tsai [5]. This design consists of TRIAX and MAT as skin materials and C260 glass/epoxy as the major structural material (Table 3). The reference fiber direction for the composite material is considered along the span direction (green arrow) and layups direction (pink arrow) can

be seen in Figure 6. All sections have same number of MAT skin material layers while individual section has different number of TRIAX and C260 materials layers (Table 4). The ANSYS ACP composite prepost [8] was used as a preprocessor for composite layups modeling as well as for post processing to check the failure criteria. The numbers of layers of C260 material for individual sections were tagged as a parameter which would be the input as the structural design variable for the optimization process.

Table 3: SERI-8 composite materials properties

Materials			
	TRIAX	C260	MAT
Density (lb/in^3)	0.085513	0.062757	0.010339
Mass Density (lb/in^3 /g /12)	0.000221	0.000163	2.68E-05
E1 (psi)	3930000	6140000	1100000
E2 (psi)	1640000	1410000	1100000
G (psi)	940000	940000	940000
Poisson's Ratio	0.3	0.3	0.3
Limit Stress Dir 1 Tension (psi)	88200	103000	19000
Limit Stress Dir 1 Compression (psi)	53100	49800	20000
Limit Stress Dir 2 Tension (psi)	13600	2300	19000
Limit Stress Dir 2 Compression (psi)	15000	2300	20000
Limit Shear Stress (psi)	15000	3600	13000
Limit Interlaminate Stress (psi)	15000	3600	13000
Thickness (in)	0.015	0.005	0.005
Cost ($/lb)	0	1.5	0

Table 4: SERI-8 composite materials and layups distribution

Station	Location (cm)	100 % Glass Fiber Model		
		MAT	TRIAX	C260
1	0-61	2	4	75(90°)
2	61-122	2	4	40(0°)
3	122-183	2	4	60(0°)
4	183-244	2	3	80(0°)
5	244-305	2	3	70(0°)
6	305-366	2	2	55(0°)
7	366-427	2	2	55(0°)
8	427-488	2	2	42(0°)
9	488-549	2	2	30(0°)
10	549-610	2	2	30(0°)
11	610-671	2	2	25(0°)
12	671-732	2	2	2(0°)
13	732-793	2	6	0

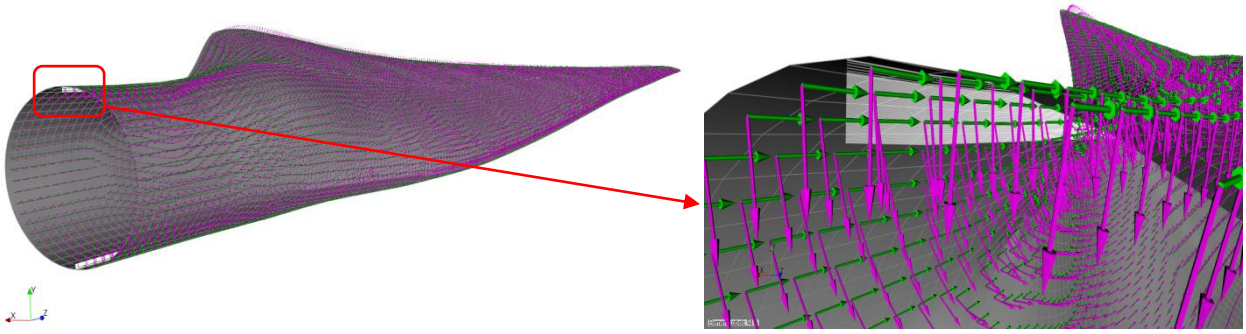

Figure 6: ANSYS ACP Prepost-composite modeling/layups

3.4 CFD Simulation

The ANSYS CFX [8] was used to perform CFD analysis of the blade. The rotating and stationary fluid domains were generated in design modeler and meshed using CFX mesh technique to generate 1.8 million tetrahedral elements. In order to simplify the CFD analysis and to save computational time, domains with 120 degree wedge model were created with one blade, assuming symmetry boundary conditions on the left and right side of the domain (Figure 7). Each side of the domain was given periodic boundary conditions [9]. It implies that the velocities going out from the left side boundary can enter the boundary on the other side in an infinite loop. It was assumed that the flow conditions on either side of the 120^0 wedge are fully symmetric.

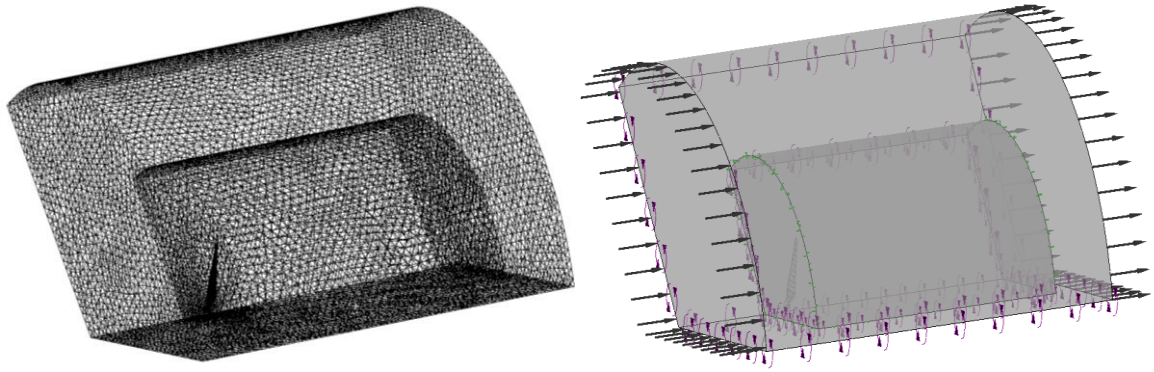

Figure 7: Fluid domain with 120^0 wedge model and boundary conditions

The flow was assumed to be ideal, steady and homogenous. A turbulence models chosen were *k-epsilon* turbulence and *k-w, SST* (shear-stress transfer) to capture the turbulence phenomena [10]. The inlet boundary condition for wind speed was set as a fixed uniform entrance velocity, a static pressure outlet boundary condition was applied with free stream wall condition and blade surfaces were defined as no slip walls with rotation. The attached angle of the blade to the hub was given as an input parameter while torque generated from the blade was tagged as an output parameter to calculate the power generated as an objective for the optimization process.

3.5 Fluid- Structure Interaction (FSI)

FSI [8] is used when there is an interaction between a solid and a fluid. The "one-way" FSI system was used. CFX calculates aerodynamic loads and were transferred to the static analysis module for structural analysis. Blade was given the clamped constraints at the root section of the blade and the tip deformation and maximum stresses were calculated from mapped pressure load on the blade from CFX. The total deformation and maximum stresses were tagged as output parameters for the optimization process. Furthermore, static analysis module was connected to the modal analysis module and the first three modal frequencies of the blade were calculated and marked as output parameters to define the constraint limits.

3.6 Cost Estimation

In this research, the cost calculation for one blade based on Ong and Tsai [5] was done. The labor cost, material cost and total cost were calculated. Assumptions were made as per Ong and Tsai's paper [5] and only major structural material C260 was used for cost estimation. Furthermore, the tooling cost was not considered in this analysis. The total labor hour for each lay-up is taken as 9.1 hours [5]. The total cost for single blade can be calculated as follows:

$$\text{Material cost} = \text{Material mass (lb)} \times \text{Material cost (\$/lb)} \quad (1)$$

$$\text{Labor cost} = \text{Total labor hours (hr)} \times \text{Labor rate (\$/hr)} \quad (2)$$

$$\text{Total cost} = \text{Material cost} + \text{Labor cost} \quad (3)$$

The total cost of the blade was calculated by defining new output parameter in ANSYS workbench [8] and mentioned as a design objective to be minimized in the optimization process.

4 Aero- Structural Optimization

It is not possible to formulate the problem of optimum design of wind turbine blades as a single-criteria optimization task because this process requires many criteria to be taken into account. In many cases, these criteria are mutually incomparable, uncountable and sometimes even contradictory, which precludes their simultaneous optimization. The following criteria have taken into account in the process of optimal wind turbine design,

- Minimize weight of the blade
- Minimize blade total cost
- Minimize blade vibration and keep modal frequency at acceptable level
- Maximize power output
- Accomplishment of appropriate strength requirements

The mass and material cost of a blade is correlated and depends on the blade structural stiffness. If the blade design robustness is at optimal level then both the criteria can be satisfied. The optimal blade thickness for different blade section helps to satisfy these criteria. Minimization of vibration is a better way to obtain optimal design of blade structure and at the same time it contributes to keep the cost low and provide high stiffness. Hence, to minimize vibration, the natural frequency of the blade should be separated from the harmonic vibration associated with rotor resonance. Therefore, mode separation constraint was setup to examine the first three natural frequencies and is separated from each other by more than ±5% of its natural frequency.
Furthermore, to meet the strength requirements of the structure, optimization of maximum displacements of the blade at the tip would have to be carried out with a limiting constraint and permissible stress should not be exceeded. To maximize a torque and hence power, blade pitch angle and shape should be optimized. Henceforth, optimal pitch angle need to be obtained to maximize the power generated.

4.1 Multidisciplinary Design Optimization

As explained earlier, the main objective of the present work was to develop a multidisciplinary design optimization procedure for SERI-8 blade. The blade needs to be optimized for optimal aerodynamic performance and structural robustness. The key objectives were to minimize mass and cost of the blade and maximize power output. The reference SERI-8 blade was aerodynamically optimized based on BEM theory with modified twist angle. The blade pitch angle was given as an input variable parameter to guarantee a good aerodynamic performance. The numbers of layups at different sections were tagged as a structural design variable.
The constraints in wind turbine blade design are as follows:

- Displacement of the blade cannot exceed the set value (global stability must be ensured),
- Maximum stresses generated in the blade cannot exceed permissible stresses (appropriate strength requirements for the structure), and
- Separation of natural frequencies of the blade from harmonic vibrations associated with rotor rotation.

The design constraints, variables and objectives for this case study are summarized in Table 5.

Table 5: Variables, constraints and objective for the MDO process

Variables	- Blade thickness (Number of layers at section 1 to 12 - ACP pre) - Blade pitch angle (CFX)
Constraints	- Blade deflection (Tip) <11 inch - Failure criteria (Tsai Wu) - Model frequency separation (±5% of natural frequency)
Objectives	- Minimize weight - Minimize cost - Minimize stresses - Maximize power output

ANSYS Workbench 14.5 [8] and design explorer module was used to carry out the multidisciplinary design optimization problem. Design exploration describes the relationship between the design variables and the performance of the blade by using Design of Experiments (DOE), combined with response surfaces and identifies the relationship between the performance of the blade and the input design variables. Once the response surface has been introduced, the optimization study needs to be defined, Central Composite Design-G optimality method was used and desired objectives and constraints were set within the specified domains.

5 Results

5.1 Baseline Design Validation

To calibrate baseline SERI-8 blade with respect to reference SERI-8 model (Ong and Tsai), the mass of each section was compared (Figure 8). The mass of baseline SERI-8 found was very close to the weight indicated in Ong and Tsai's model [5] and the percentage difference was found to be 0.70%.

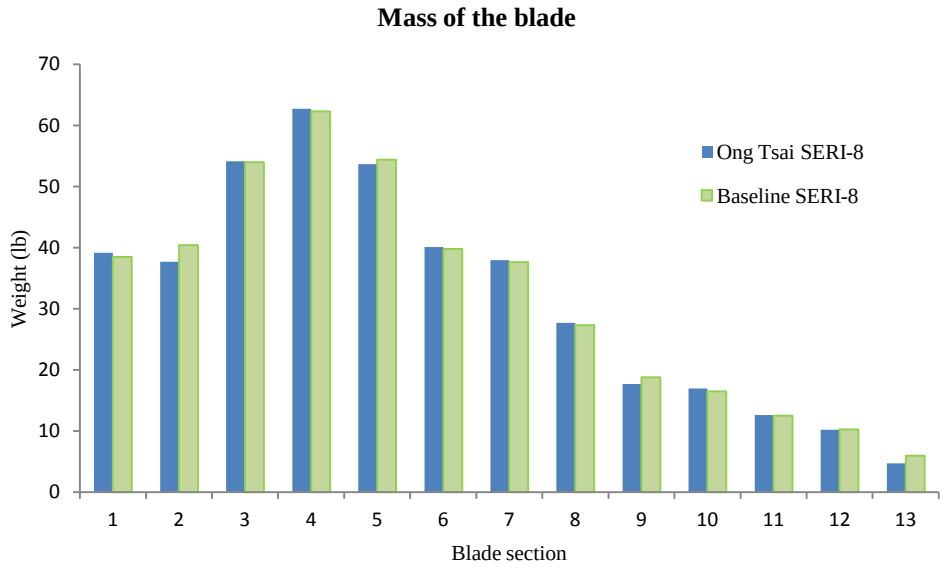

Figure 8: Mass comparison of reference and baseline SERI-8 blades

The total single blade cost for reference SERI-8 and baseline SERI-8 blade is shown in Figure 9. The variation in total cost between both blades was found to be 1.5%. This calculation was done based on similar cost values used by Ong and Tsai[5] for the validation purpose which may vary based on present material cost and labor cost values.

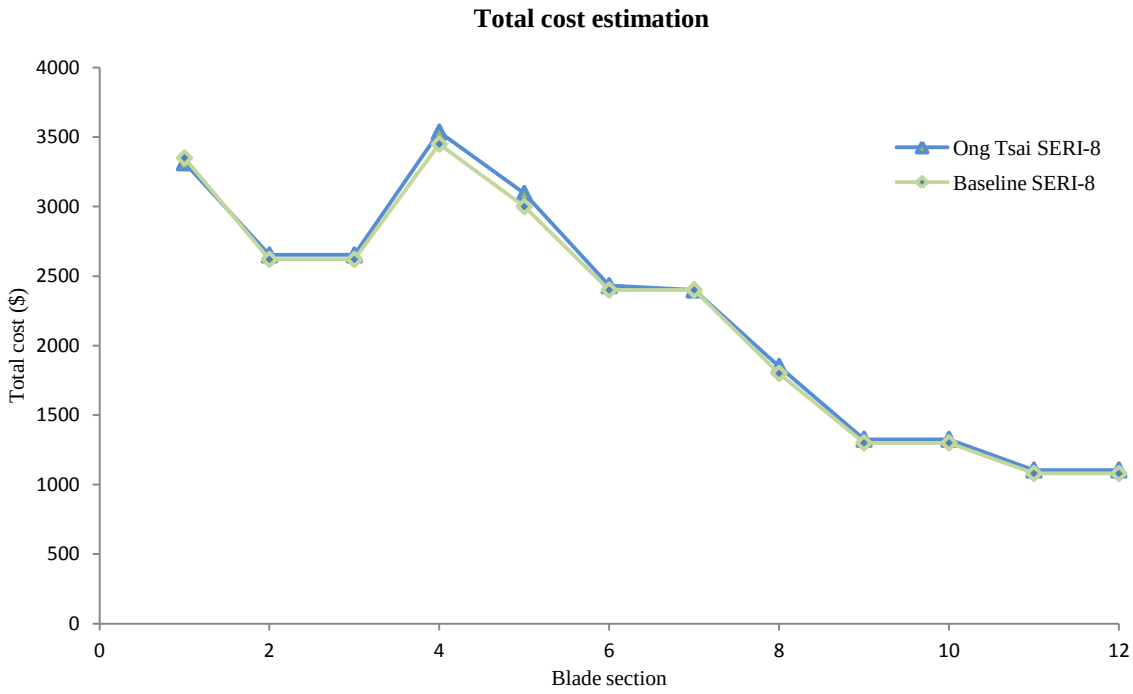

Figure 9: Total cost comparison of reference and baseline SERI-8

5.2 CFD Simulation

A steady state solution with *k-epsilon* turbulence model was solved in ANSYS CFX for both baseline and modified SERI-8 blades. The results are obtained at five different wind speeds and compared in terms of flow separation, pressure distribution and power production. The power production results are shown in Table 5. For better comparison, the power curve for baseline SERI-8 need to be compared with the experimental data. Therefore, an available experimental result of SERI-9 blade (which has same airfoils sections and length of 9.2 m [11]) was scaled down to compare with SERI-8 power curve. It can be seen from (Figure 10), that the power curve for scaled SERI-9 and baseline SERI-8 has a similar pattern. Furthermore, it can be observed that power produced by modified new SERI-8 is higher in range of 1 to 3 % compared to the baseline SERI-8 design at the operating wind speed range (Table 6).

Table 6: Torque and power output for baseline and new SERI-8 blade designs

	Baseline Design		**New SERI-8_Qblade**		
Wind speed	Torque Nm)	Power (kw)	Torque Nm)	Power (kw)	**Power %**
5	650	6.64	670	6.84	**3.08**
10	3400	34.71	3520	35.94	**3.53**
15	5560	56.77	5730	58.50	**3.06**
20	6610	67.49	6730	68.71	**1.82**

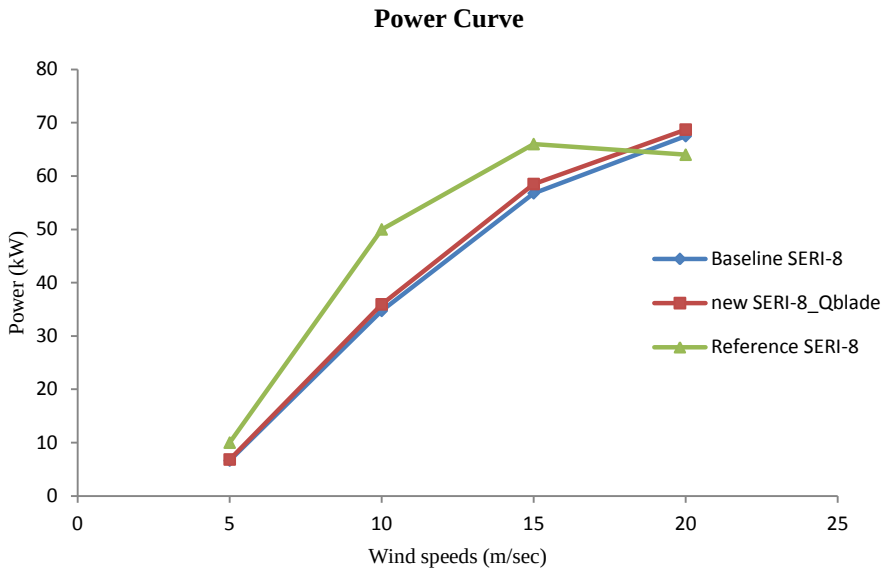

Figure 10: Power curve of SERI-8 blades

Figure 11 shows that the streamlines of SERI-8 blade at 25%, 50%, 75% and 95% of blade lengths. It can be observed that the vortices due to turbulence and flow separation at the trailing edge are generated. This may cause less torque and power generation. In contrast, modified SERI-8 blade (Figure 12) has no flow separation at any section corresponding to 25%, 50%, 75% and 95% of the blade lengths and a fully attached flow present helps to generate a higher torque and power output.

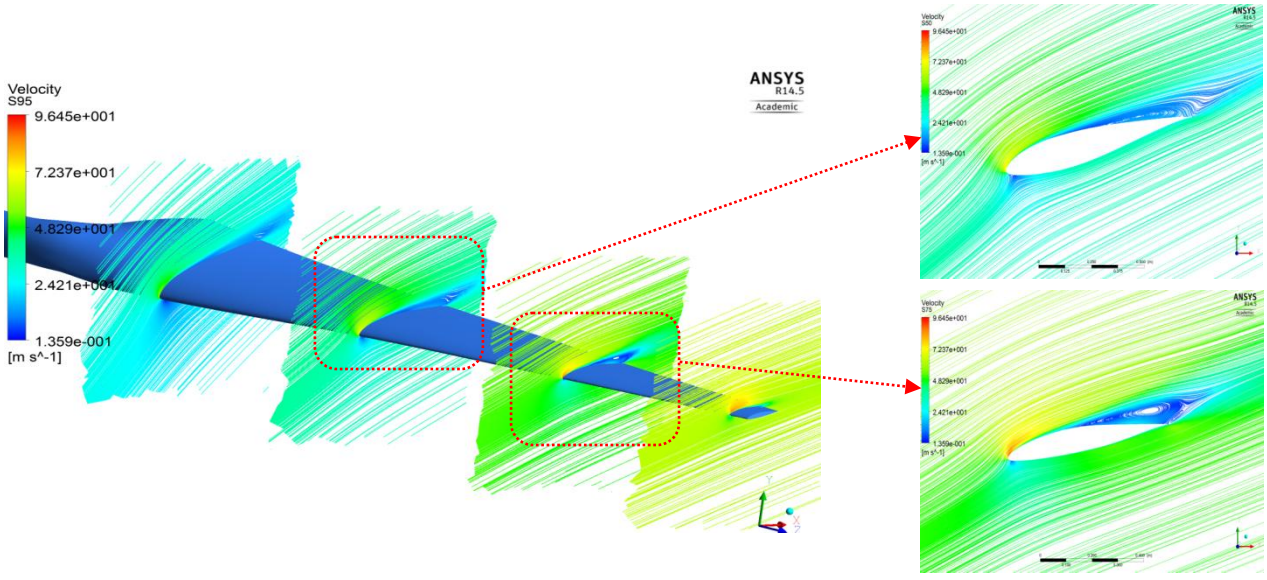

Figure 11: Baseline SERI-8 blade, streamlines at different section at 20 m/s wind speed

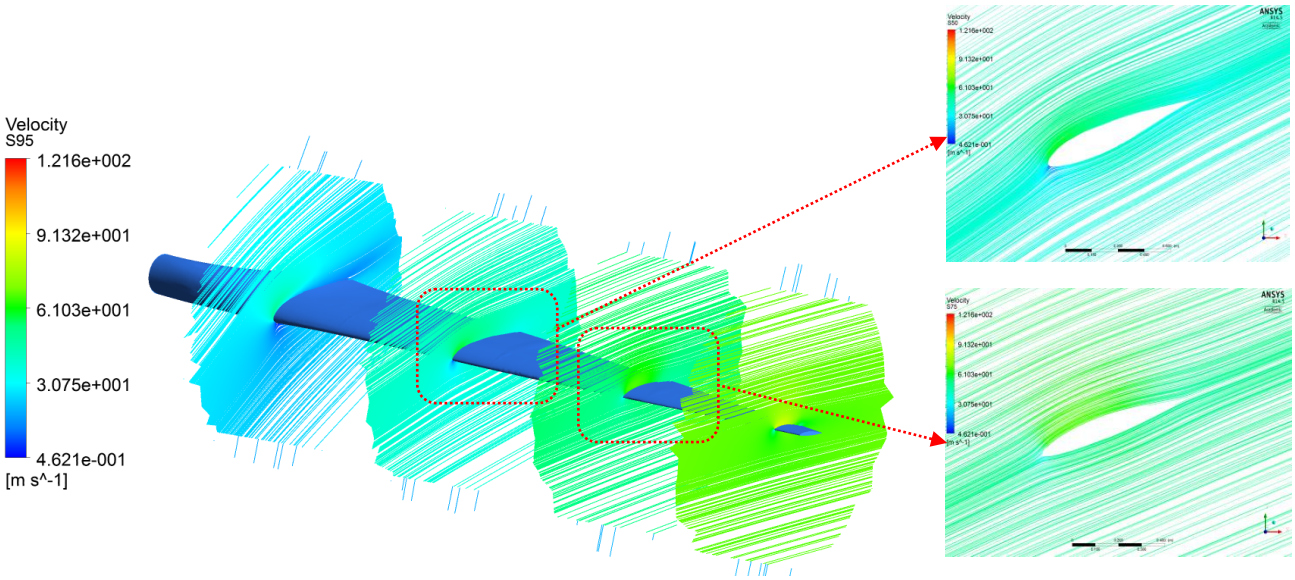

Figure 12: New SERI-8 blade, streamlines at different section at 20 m/s wind speed

5.3 Optimization

For new SERI-8 blade, 281 DOEs were solved and a response surface was generated. Based on the created responses, 1000 design candidates were produced within the pre-defined minimum and maximum values for variable parameters. Multi objectives and constraints were set with kriging algorithm. This provides an improved response quality and fits higher order variations of the output parameter and all design candidates were analyzed.

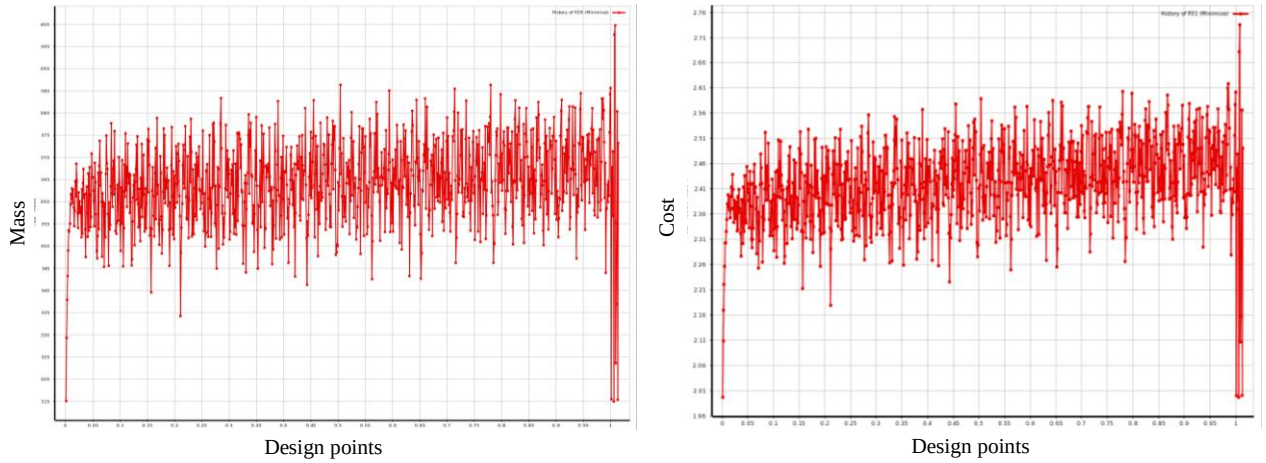

Figure 13: Objective parameters versus design points

Figure 13, shows value of objective parameters at each design point. Figure 14 shows tradoff chart for two objectives, total cost and total mass. It can be observed that cost and mass of the blade is propostional to each. It also indicats feasible and infeasible points (which were filtered based on constraint values).

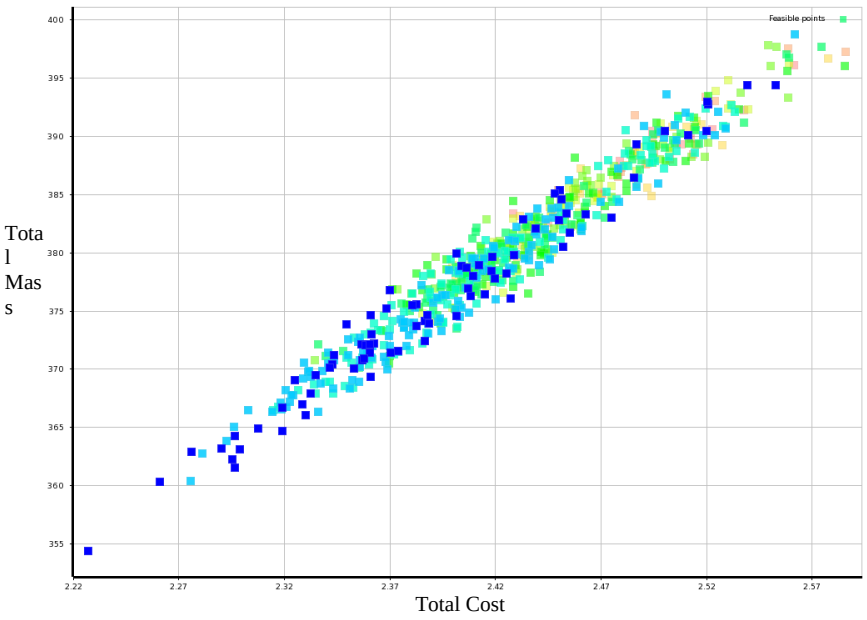

Figure 14: Tradeoff chart of total mass versus total cost

Figure 15 shows a tradeoff chart of total cost (objective) versus total deformation (constraint). The constraint limit was set less than 11 inches and all of the design points above this value were marked as infeasible points and remaining were feasible design points. Similar phenomena can be seen in tradeoff chart for maximum stress (objective) versus total deformation (constraint) and all of the design points with total deformation value above 11 inches were separated as infeasible design points.

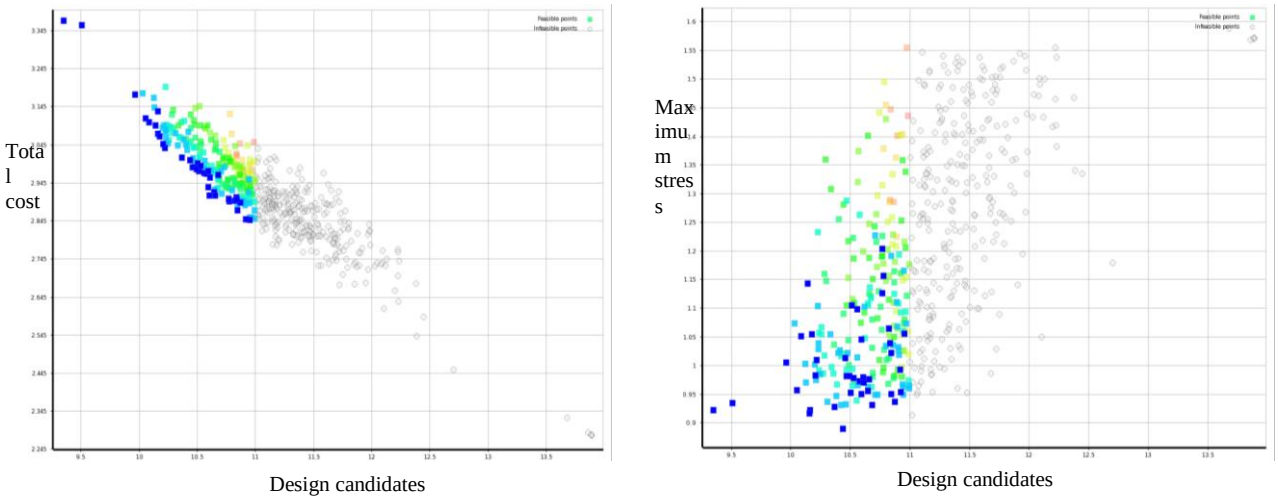

Figure 15: Tradeoff charts of objective versus constraint

Table 7 shows top 3 optimum feasible design candidates.

Table 7: Optimum design candidates

			Candidate 1	Candidate 2	Candidate 3
Input parameters	Number of layers	Section 1	60	61	63
		Section 2	30	38	33
		Section 3	50	55	53
		Section 4	65	68	69
		Section 5	64	57	61
		Section 6	41	41	44
		Section 7	40	41	41
		Section 8	30	31	33
		Section 9	25	20	23
		Section 10	22	22	31
		Section 11	17	15	18
		Section 12	15	16	15
	Blade pitch angle (°)		7	10	10
Output parameters	Total deformation (in)		10.97	8.56	8.12
	Maximum stress (psi)		5751.98	5610.58	5520.35
	Total mass (lb.)		315.03	329.34	339.59
	Total cost ($)		19966	21082	22129
	Power (kW)		58.65	45.51	45.86
	Model Frequency 1		4.46	4.54	4.45
	Model Frequency 2		7.97	8.19	8.20
	Model Frequency 3		12.80	12.95	12.99

In addition, local sensitivity chart for this MDO process is shown in Figure 16. Local sensitivity chart is plotted to observe the impact of input parameters on output parameters. It calculates the change of the output(s) based on the change of inputs independently at the current value of each input parameter. The larger the change of the output parameter(s), the more significant is the role of the input parameters that were varied. It can be observed that first three blade sections (input parameter) have maximum impact on most output parameters. These sensitive parameters can be treated accordingly to minimize critical impact of individual input parameters. It also drives attention to mid sections of the blade as the maximum blade torque is generated at this region and local sensitivity curve shows significant impact on blade deformation and stress values. Therefore, it is important to carefully design each section of the blade for better aerodynamic performance and for structural robustness.

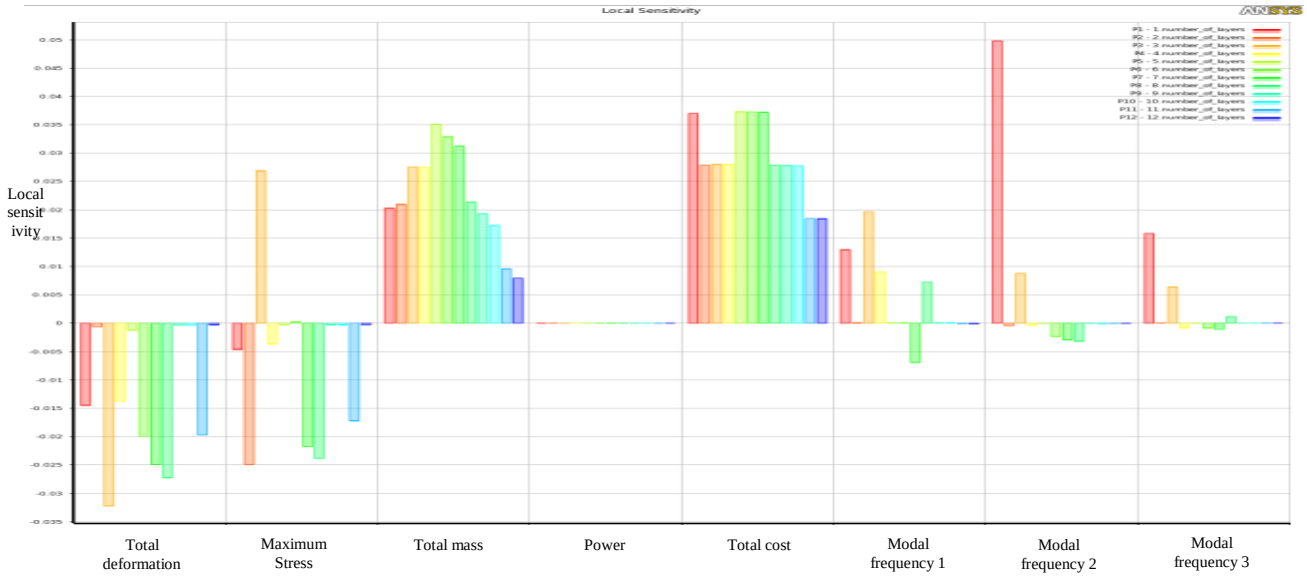

Figure 16: Local sensitivity of input parameters to output parameters

As results from MDO process (Table 8), Candidate 1 values were used to check the aerodynamic performance and the structural strength of the optimized design. Table 8 shows a comparison between baseline and optimized SERI-8 blade. Figure 17 shows the pressure distribution on the blade at different sections which is higher than the baseline model and is significantly improved. Additionally, composite failure criteria for critical layer can be seen in Figure 18 for pressure and suction side with inverse and reverse failure factors respectively which are within a failure limit.

Table 8: Comparison of baseline design and optimum design

			Baseline Design	**Optimum Design**	
Input Parameters	Number of Layers	Section 1	75	60	
		Section 2	60	30	
		Section 3	60	50	
		Section 4	80	65	
		Section 5	70	64	
		Section 6	55	41	
		Section 7	55	40	
		Section 8	42	30	
		Section 9	30	25	
		Section 10	30	22	
		Section 11	25	17	
		Section 12	25	15	
	Blade pitch angle (degree)		9.58	7	
Output Parameters	Total deformation (in)		13.56	10.85	**19.98 % (-)**
	Maximum stress (psi)		6532.52	5725.21	**12.35 % (-)**
	Total mass (lb.)		412.68	315.03	**23.67 % (-)**
	Total cost ($)		27448	19966	**27.25 % (-)**
	Power (kW)		56.77	58.65	**3.31 % (+)**
	Model Frequency 1		4.46	4.43	
	Model Frequency 2		7.97	7.91	
	Model Frequency 3		12.80	12.77	

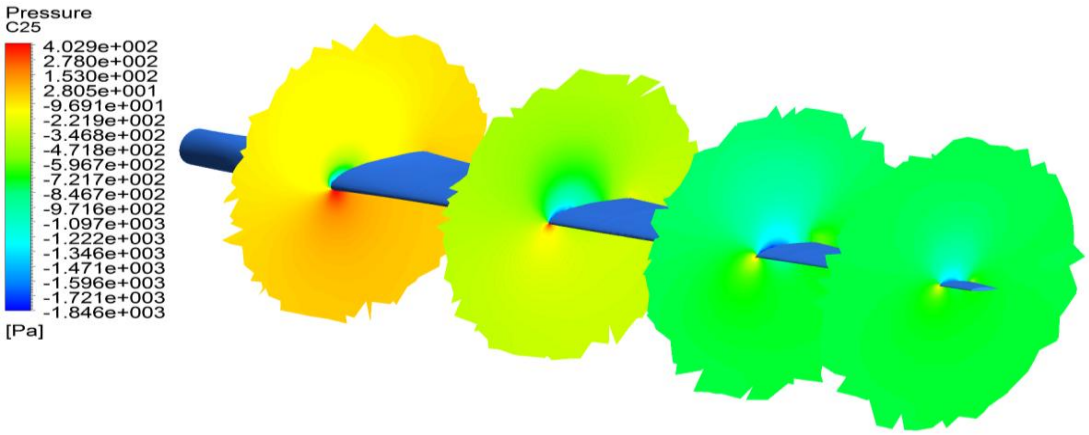

Figure 17: Optimized SERI-8 blade: Pressure contour at different section at 15 m/s wind speed

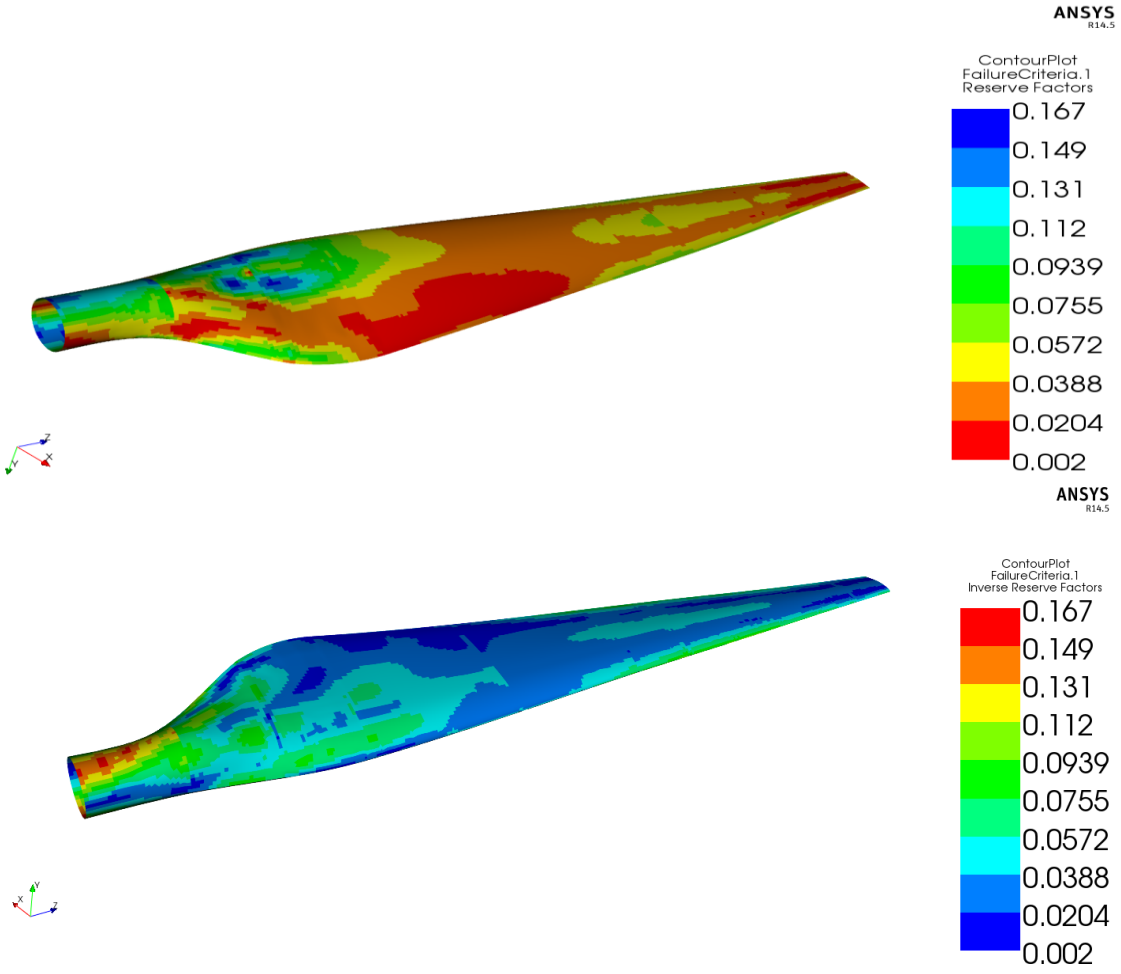

Figure 18: Optimized SERI-8: Composite failure criteria

6 Conclusion

Aero-structure multidisciplinary optimization process is carried out for SERI-8 blade using Qblade for 2D aerodynamic analysis and ANSYS workbench for 3D aerodynamic and structural analysis. It can be seen that every single objective cannot simultaneously reach the optimum in multidisciplinary objective optimization, but a compromise among the objectives is needed. The aerodynamic performance of the optimized wind turbine design is improved by about 4% compared to the baseline design. In addition the following were observed in the optimized design: mass reduction of 23.67%, cost reduction of 27.25%, reduction of maximum deformation of 19.98% and maximum stress reduction of 12.35%.

This complex MDO process presented here can be applied to the design of wind turbine blades to obtain a structurally optimized blade design with optimal blade thickness distribution and maximum power output without compromising its aerodynamic performance.

Acknowledgements

The authors wish to thank Dr. Somnath Nagendra for all his guidance and help throughout the course of this research project. Thanks are to Embry-Riddle Aeronautical University for providing the resources needed for this research.

References

[1] T. E. W. E. Association, Pure Power-Wind Energy Scenarios Upto 2030, March-2008.

[2] J. Logan and M. K. Stan , "Wind Power in the United States: Technology, Economic, and Policy Issues," June 20, 2008.

[3] T. Berlin, "Qblade," [Online]. Available: http://qblade.de.to/.

[4] Dassault Systems, "CATIA," France.

[5] S. Tsai and C. H. Ong, "The Use of Carbon Fiber in Wind Turbine Blade Design: A SERI-8 Blade Example," Sandia National Labs, March 1, 2000.

[6] J. W. Lee and S. N. Gangadharan, "Multidisciplinary Design Optimization of a Hybrid Composite Wind Turbine Blade," 2011.

[7] B. Kim, K. Woojune, B. Sungyoul, P. Jaehyung and K. Manneung, "Aerodynamic Design and Performance Analysis of Multi-MW Class Wind Turbine Blade," vol. 25, no. 8, April 24, 2011.

[8] "ANSYS Workbench," 1970.

[9] D. Digraskar, "Simulations of Flow Over Wind Turbines," University of Massachusetts, Amherst, May 2010.

[10] C. E. Carcangiu, "CFD-RANS Study of Horizontal Axis Wind Turbines," January 2008.

[11] J. Tangler, B. Smith, N. Kelley and D. Jager, "Measured and Predicated Rotor Performance for the SERI Advanced Wind Turbine Blades," February 1992.

[12] Gujicic, M.; Arakere, G.; Sellappan, V.; Vallejo, A.; Ozen, M., "Multidisciplinary Design Optimization for Glass-Fiber Epoxy-Matrix Composite 5 MW Horizontal-Axis Wind-Turbine Blades",2009.

[13] R.B. Langtry, J.Gola, and F.R. Menter, "Predicting 2D airfoil and 3D Wind Turbine Rotor Performance Using a Transition Model for General CFD Codes," AIAA 2006-0395.